Available online at www.sciencedirect.com
SCIENCE DIRECT®
PERGAMON
Chaos, Solitons and Fractals 19 (2004) 569–579
CHAOS
SOLITONS & FRACTALS
www.elsevier.com/locate/chaos

Calculation of Lyapunov exponents in systems with impacts

Silvio L.T. de Souza *, Iberê L. Caldas

Instituto de Física, Universidade de São Paulo, C.P. 66318, 05315-970 São Paulo, SP, Brazil

Accepted 24 March 2003

Communicated by T. Kapitaniak

Abstract

We apply a model based algorithm for the calculation of the spectrum of the Lyapunov exponents of attractors of mechanical systems with impacts. For that, we introduce the transcendental maps that describe solutions of integrable differential equations, between impacts, supplemented by transition conditions at the instants of impacts. We apply this procedure to an impact oscillator and to an impact-pair system (with periodic and chaotic driving). In order to show the method precision, for large parameters range, we calculate Lyapunov exponents to classify attractors observed in bifurcation diagrams. In addition, we characterize the system dynamics by the largest Lyapunov exponent diagram in the parameter space.

1. Introduction

Lyapunov exponents characterize dynamical system attractors and their initial sensitivity for initial conditions [1]. They measure the average divergence or convergence of nearby trajectories along certain directions in phase space. If the largest Lyapunov exponent is positive (non-positive) the attractor is chaotic (regular).

Consequently, Lyapunov exponents are useful to characterize bifurcation and chaos that are common as nonlinear effects in mechanical systems with impacts [2–4].

The spectrum of Lyapunov exponents has been calculated for many smooth, continuous systems described by differential equation of motion and for discrete maps described by difference equations [5–7]. But, if a system under consideration is non-smooth, the calculation of Lyapunov exponents is not straightforward [8]. In recent years several methods for this calculation have been proposed [9–11].

In this work we consider an impact oscillator [12,13] and an impact-pair system [14] (with periodic and chaotic excitation) for which the trajectories in phase space have discontinuities caused by the impacts. Due to these discontinuities we cannot use the classical algorithms applied to compute Lyapunov exponents of smooth systems. To compute the Lyapunov exponents in the impact systems we introduce transcendental maps with dynamical variables defined at the impact instants [14,15]. These maps describe solutions of the integrable differential equations, between impacts, supplemented by transition conditions at the instants of impacts. With such maps, we introduce an algorithm similar to those used to compute the Lyapunov exponents of classical smooth maps, as the Hénon map [16,17].

To show the method precision of the algorithm proposed, for large parameters range, we use the calculated Lyapunov exponents to classify attractors observed in bifurcation diagrams. In addition, we characterize the system dynamics by the largest Lyapunov exponent diagram in the parameter space.

* Corresponding author.
E-mail addresses: thomaz@if.usp.br (S.L.T. de Souza), ibere@if.usp.br (I.L. Caldas).

0960-0779/$ - see front matter © 2003 Elsevier Ltd. All rights reserved.
doi:10.1016/S0960-0779(03)00130-9

This paper is organized as follows: in the second section we describe the mathematical models of the systems and introduce the transcendental maps. In Section 3 we present how to calculate the Lyapunov exponents using a transcendental map and show numerical results of this calculation. Our conclusions are presented in Section 4.

2. Mathematical description and transcendental maps

2.1. Impact oscillator

The impact oscillator [12] shown in Fig. 1 is composed of a periodically forced oscillator with a unilateral amplitude constraint.

The motion of this system is a combination of smooth motion governed by a linear differential equation interrupted by a series of non-smooth impacts.

The smooth motion is described by the equation

$$\ddot{x} + x = \alpha\cos(\omega t), \quad x < x_c \tag{1}$$

where x_c, α and ω are the amplitude constraint, the forcing amplitude and the forcing frequency, respectively.

Integrating Eq. (1) and invoking initial condition ($x(t_0) = x_0$, $\dot{x}(t_0) = \dot{x}_0$), the displacement x and the velocity $\dot{x}$ between impacts are

$$x = \left[x_0 - \frac{\alpha}{(1-\omega^2)}\cos(\omega t_0)\right]\cos(t - t_0) + \left[\dot{x}_0 + \frac{\alpha\omega}{(1-\omega^2)}\sin(\omega t_0)\right]\sin(t - t_0) + \frac{\alpha}{(1-\omega^2)}\cos(\omega t) \tag{2}$$

$$\dot{x} = \left[-x_0 + \frac{\alpha}{(1-\omega^2)}\cos(\omega t_0)\right]\sin(t - t_0) + \left[\dot{x}_0 + \frac{\alpha\omega}{(1-\omega^2)}\sin(\omega t_0)\right]\cos(t - t_0) - \frac{\alpha\omega}{(1-\omega^2)}\sin(\omega t) \tag{3}$$

An impact occurs wherever $x = x_c$ (amplitude constraint). After each impact, we apply into Eqs. (2) and (3) the Newton law of impact

$$\begin{aligned} t_0 &= t \\ x_0 &= x \\ \dot{x}_0 &= -r\dot{x} \end{aligned} \tag{4}$$

where r is a constant coefficient of restitution.

Thus, the evolution of the impact oscillator is given by Eqs. (2)–(4). Consequently, the system depends on the control parameters x_c, α, ω, and r.

From these equations, varying the control parameters in our numerical simulations, we observe both periodic and chaotic attractors. For instance, Fig. 2a shows the evolution of a regular (periodic) solution while Fig. 2b shows an irregular (chaotic) solution. It is interesting to observe in these figures jumps in the velocity, $\dot{x}$, evolution. These jumps, represented by dashed lines, correspond to the discontinuity of trajectories caused by impacts. Due to these discontinuities we cannot use the algorithms usually applied to compute Lyapunov exponents in smooth systems (once derivatives at the impact, required to calculate such exponents, are not defined). To overcome this problem we introduce next a transcendental map to develop an adapted algorithm that can be applied to the impact oscillator system described in this section.

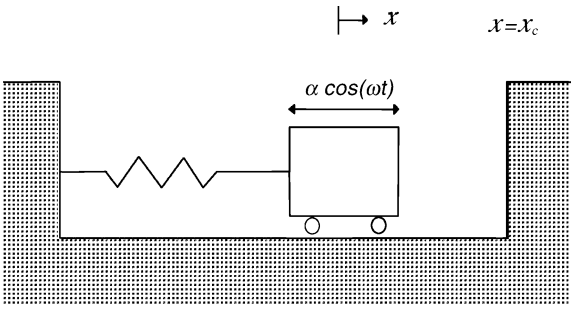

Fig. 1. Model of an impact oscillator.

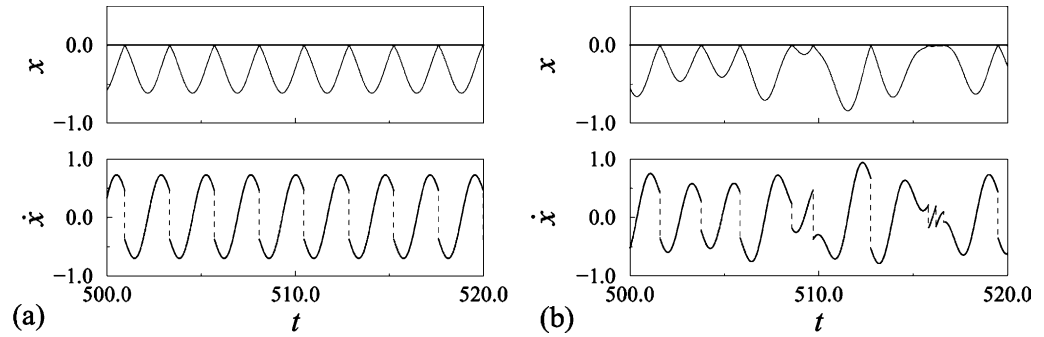

Fig. 2. The impact oscillator for the control parameters $\alpha = 1.0$, $r = 0.8$, and $x_c = 0$. Displacement, x, and velocity, $\dot{x}$, as a function of the time, t, for a periodic attractor (a) with $\omega = 2.64$ and a chaotic attractor (b) with $\omega = 2.8$.

To obtain the transcendental map, we consider the variables x_n, $\dot{x}_n$, and t_n computed just before the impact n. The variables x_{n+1}, $\dot{x}_{n+1}$ and t_{n+1} are obtained from Eqs. (2) and (3) for the initial conditions:

$$\begin{aligned} t_0 &= t_n \\ x_0 &= x_n \\ \dot{x}_0 &= -r\dot{x}_n \end{aligned} \tag{5}$$

Thus, we can introduce the transcendental map (obtained from Eqs. (2), (3), and (5)):

$$\begin{aligned} x_{n+1} &= \left[x_n - \frac{\alpha}{(1-\omega^2)}\cos(\omega t_n)\right]\cos(t_{n+1}-t_n) + \left[-r\dot{x}_n + \frac{\alpha\omega}{(1-\omega^2)}\sin(\omega t_n)\right]\sin(t_{n+1}-t_n) + \frac{\alpha}{(1-\omega^2)}\cos(\omega t_{n+1}) \\ \dot{x}_{n+1} &= \left[-x_n + \frac{\alpha}{(1-\omega^2)}\cos(\omega t_n)\right]\sin(t_{n+1}-t_n) + \left[-r\dot{x}_n + \frac{\alpha\omega}{(1-\omega^2)}\sin(\omega t_n)\right]\cos(t_{n+1}-t_n) - \frac{\alpha\omega}{(1-\omega^2)}\sin(\omega t_{n+1}) \end{aligned} \tag{6}$$

where $x_{n+1} = x_n = x_c$.

Using Eq. (6) we develop the algorithm used to obtain the Lyapunov exponents.

2.2. Impact-pair system

Fig. 3 depicts the mechanical model of the impact-pair system [14]. The system is composed of a point mass m (where displacement is denoted by x) and a box (displacement $e(t)$) with a gap of length v. The mass m is free to move inside the gap. The motion of the box can be periodic, quasi-periodic or chaotic.

In this work, we consider both periodic and chaotic motion of the box. For the periodic case, we use $e(t) = \alpha\sin(\omega t)$ and the chaotic one $e(t)$ is obtained from a chaotic solution of the Duffing's equation

$$\ddot{e} - e + e^3 + c\dot{e} = \alpha\cos(\omega t) \tag{7}$$

where c, α, ω are the damping, the forcing amplitude, and the forcing frequency, respectively.

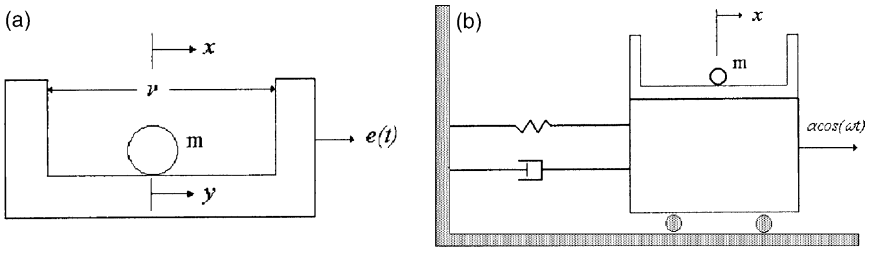

Fig. 3. (a) Model of an impact-pair system. (b) Model of the impact-pair system whose energy source is given by a solution of the Duffing's equation.

Our model with chaotic excitation is presented in Fig. 3b. We consider a massive cart, whose motion is described by Duffing's equation and is not affected by impacts. In this case, the impact-pair system is in the upper part of the cart. Eq. (7) is solved numerically by the Runge–Kutta method of order 4.

The motion of the point mass m in the absolute coordinate system is described by the solution of the homogeneous equation

$$\ddot{x} = 0 \tag{8}$$

Integrating Eq. (8) and invoking initial conditions ($x(t_0) = x_0$ and $\dot{x}(t_0) = \dot{x}_0$), the displacement x and velocity $\dot{x}$, between impacts, are

$$x(t) = x_0 + (t - t_0)\dot{x}_0 \tag{9}$$

$$\dot{x}(t) = \dot{x}_0 \tag{10}$$

Denoting the relative displacement y of the mass m, we have

$$x = y + e(t) \tag{11}$$

Substituting Eq. (11) into Eqs. (9) and (10), the solution is given by

$$y(t) = y_0 + e(t_0) - e(t) + [\dot{y}_0 + \dot{e}(t_0)](t - t_0) \tag{12}$$

$$\dot{y}(t) = \dot{y}_0 + \dot{e}(t_0) - \dot{e}(t) \tag{13}$$

An impact occurs wherever $y = v/2$ or $-v/2$. After each impact, we apply into Eqs. (12) and (13) the new set of initial conditions (the Newton law of impact)

$$\begin{aligned} t_0 &= t \\ y_0 &= y \\ \dot{y}_0 &= -r\dot{y} \end{aligned} \tag{14}$$

where r is a coefficient of restitution.

Therefore, the dynamic of the impact-pair system is governed by Eqs. (12)–(14). In the case of periodic excitation ($e(t) = \alpha\sin(\omega t)$) the control parameters are v, r, α, and ω. For the chaotic excitation ($\ddot{e} - e + e^3 + c\dot{e} = \alpha\cos(\omega t)$), the parameters are v, r, c, α, and ω. Varying the parameters we identify both periodic and chaotic attractors.

For the periodic excitation, Fig. 4a shows a regular (periodic) solution while Fig. 5a shows an irregular (chaotic) solution, where heavy lines represent the position of the boundaries (walls) of the gap and the thin lines the position of the free point mass. Furthermore, in Figs. 4b and 5b we can see discontinuities (dashed lines) of the trajectories due to impacts, creating a difficult to calculate the Lyapunov exponents. Thus, as we did in Section 2.1, we also introduce a transcendental map to compute the Lyapunov exponents. Finally, for the Duffing chaotic excitation, Fig. 6 shows a possible chaotic solution.

In order to obtain the transcendental map, we use the analytical solution (Eqs. (12) and (13)) and the Newton law of impact. Thus, we have

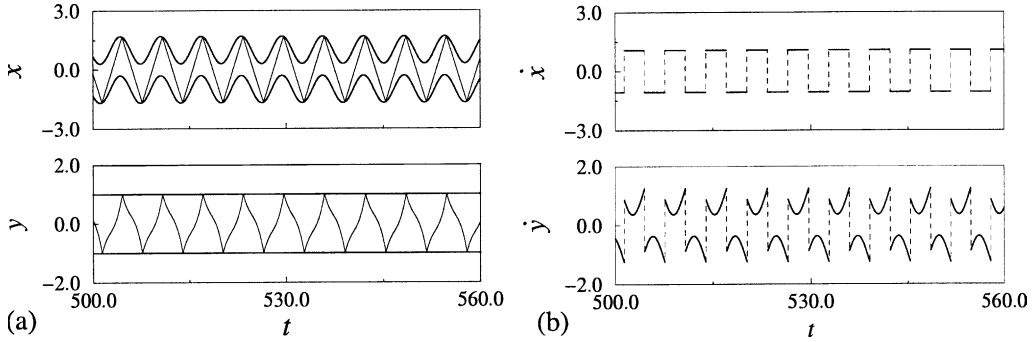

Fig. 4. Periodic attractor of the impact-pair system with $e(t) = \alpha\sin(\omega t)$ ($\alpha = 0.75$, $\omega = 1.0$, $v = 2.0$, and $r = 0.7$). (a) Absolute, x, and relative, y, displacements as a function of the time. (b) Absolute, $\dot{x}$, and relative, $\dot{y}$, velocity evolution.

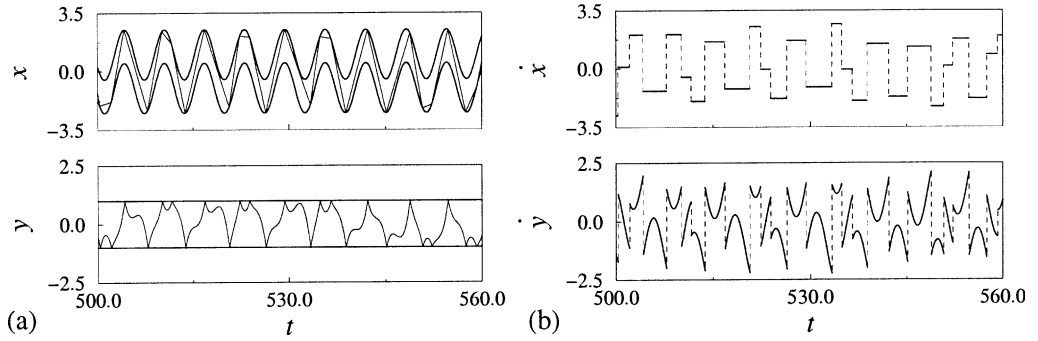

Fig. 5. Chaotic attractor of the impact-pair system with $e(t) = \alpha\sin(\omega t)$ ($\alpha = 1.5$, $\omega = 1.0$, $v = 2.0$, and $r = 0.7$). (a) Absolute, x, and relative, y, displacements as a function of the time, t. (b) Absolute, $\dot{x}$, and relative, $\dot{y}$, velocity evolution.

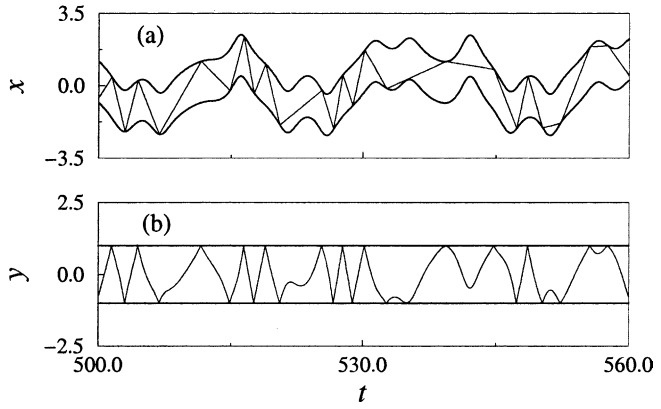

Fig. 6. Chaotic attractor of the impact pair system with $e(t)$ given by a chaotic solution of the Duffing's equation ($v = 2.0$, $r = 0.9$, $c = 0.25$, $\alpha = 0.3$, and $\omega = 1.0$). Absolute, x, (a) and relative, y, (b) displacements as a function of the time, t.

$$\begin{aligned} y_{n+1} &= y_n + e(t_n) - e(t_{n+1}) + [-r\dot{y}_n + \dot{e}(t_n)](t_{n+1} - t_n) \\ \dot{y}_{n+1} &= -r\dot{y}_n + \dot{e}(t_n) - \dot{e}(t_{n+1}) \end{aligned} \tag{15}$$

where $y_n = v/2$ or $-v/2$.

Using Eq. (15) we develop the algorithm used to obtain the Lyapunov exponents.

3. Lyapunov exponents

In this section we describe the computation algorithm to calculate the Lyapunov exponents in mechanical systems with impacts using a transcendental map. In such situation the calculation is done in the similar way of classical maps, as Hénon map.

For the considered systems, the transcendental maps are two-dimensional. In this case, the Lyapunov exponents are expressed by [18,19]

$$\lambda_j = \lim_{N\to\infty} \frac{1}{N} \ln |\Lambda_j^N|, \quad j = 1, 2 \tag{16}$$

where $|\Lambda_j^N|$ are eigenvalues of the matrix M, that is given by

$$M = \prod_{n=1}^{N} J^n \tag{17}$$

and J^n is the Jacobian matrix of the nth iteration (impact) of the transcendental map.

However, in the computation algorithm we cannot use the expression (16) because of the product (17) required to obtain the matrix M. Even for a few iterations, the components of matrix M become very large for chaotic attractors and null for the periodic attractors. Consequently, the numerical calculation become impracticable.

To eliminate this problem, we must avoid to use the product of expression (16). For that, we may convert the matrix M into a product of the orthogonal matrices and the upper right triangular matrices, as shown in Ref. [7]. In this way, the matrix M is transformed in product of the upper right triangular matrices, whose eigenvalues are the numbers along the diagonal and the Lyapunov exponents can be expressed by

$$\lambda_j = \lim_{N\to\infty} \frac{1}{N} \sum_{n=1}^{N} \ln |a_j^n|, \quad j = 1, 2 \tag{18}$$

where a_j^n are diagonal components of nth iteration of the product of the upper right triangular matrices. Thus, the Lyapunov exponents are obtained from a sum in (18) instead of a product.

Furthermore, we cannot perform exactly the infinite sum in (18) for numerical calculations, but the convergence of the Lyapunov exponents occurs with good precision after just a few thousand iterations, both for periodic and chaotic attractors.

For the mechanical systems with impacts considered in this work, the discontinuites in the trajectory have to be supplemented with transition conditions at the impact instants, t_n. Such instants are determined by integrating the equations of motion in continuous time. The value of t_n and the corresponding velocity at this time as the dynamical variables of the transcendental maps (6) and (15). Using these maps we obtain the Jacobian matrix components necessary to calculate the Lyapunov exponents.

3.1. Impact oscillator

We show here some numerical results of the calculation of the Lyapunov exponents for the impact oscillator.

To calculate the Lyapunov exponents, as mentioned earlier, we use the Jacobian matrix, J^n, of the transcendental map

$$J^n \equiv \begin{pmatrix} \frac{\partial t_{n+1}}{\partial t_n} & \frac{\partial t_{n+1}}{\partial \dot{x}_n} \\ \frac{\partial \dot{x}_{n+1}}{\partial t_n} & \frac{\partial \dot{x}_{n+1}}{\partial \dot{x}_n} \end{pmatrix} \tag{19}$$

whose components are

$$\begin{aligned} \frac{\partial t_{n+1}}{\partial t_n} &= \frac{1}{\dot{x}_{n+1}} [-x_n + \alpha\cos(\omega t_n)] \sin(t_{n+1} - t_n) - r\dot{x}_n \cos(t_{n+1} - t_n) \\ \frac{\partial t_{n+1}}{\partial \dot{x}_n} &= \frac{1}{\dot{x}_{n+1}} [r \sin(t_{n+1} - t_n)] \\ \frac{\partial \dot{x}_{n+1}}{\partial t_n} &= \frac{\partial t_{n+1}}{\partial t_n} [-x_{n+1} + \alpha\cos(\omega t_{n+1})] + [x_n - \alpha\cos(\omega t_n)] \cos(t_{n+1} - t_n) - r\dot{x}_n \sin(t_{n+1} - t_n) \\ \frac{\partial \dot{x}_{n+1}}{\partial x_n} &= \frac{\partial t_{n+1}}{\partial \dot{x}_n} [-x_{n+1} + \alpha\cos(\omega t_{n+1})] - r\cos(t_{n+1} - t_n) \end{aligned} \tag{20}$$

In Fig. 7a, we plot the phase plane of the periodic attractor seen in Fig. 2a. Fig. 7b shows the test of the convergent series of the two negative Lyapunov exponents $\lambda_{1,2}$ of this attractor, whose values are so closed that cannot be distinguished in this figure. As can be seen, the convergence occurs with good precision. To obtain the series, we use 20,000 iterations (impacts) and consider 5000 iterations as transient.

As an example of chaotic behavior, we present in Fig. 8 an attractor whose time evolution is shown in Fig. 2b. The phase plane is plotted in Fig. 8a and the test of convergent series of two Lyapunov exponents in Fig. 8b. In this figure, we can observe that one of the Lyapunov exponents is positive, what that confirms the attractor is chaotic. Besides, we note again the convergence occurs with good precision.

To show the efficiency of our algorithm for a wide range of a control parameter, we plot a bifurcation diagram (Fig. 9a) and the corresponding Lyapunov exponents (Fig. 9b). We use here a transient with 1000 iterations and 5000 iterations for the exponents calculation. Thus, we can note there is an excellent agreement between the attractor behavior shown in bifurcation diagram and their corresponding largest Lyapunov exponent values.

Fig. 10 shows a diagram of the largest Lyapunov exponents in the control parameter space. This picture is constructed using a grid of an equally spaced 400×400 points of two parameters, namely, the amplitude α and the fre-

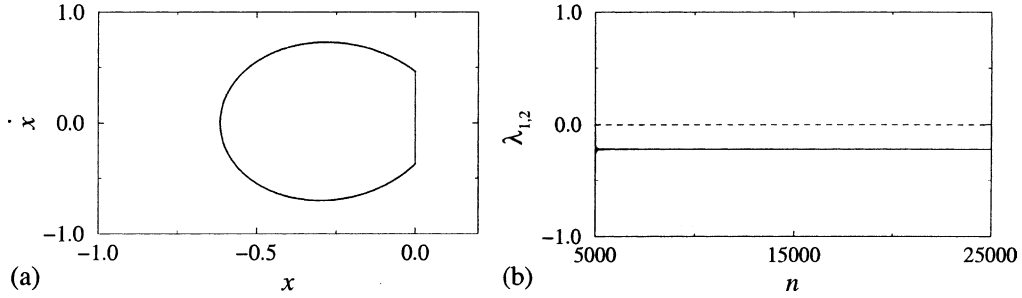

Fig. 7. (a) The phase plane of the periodic behavior shown in Fig. 2a. (b) The convergent series of the Lyapunov exponents, $\lambda_{1,2}$.

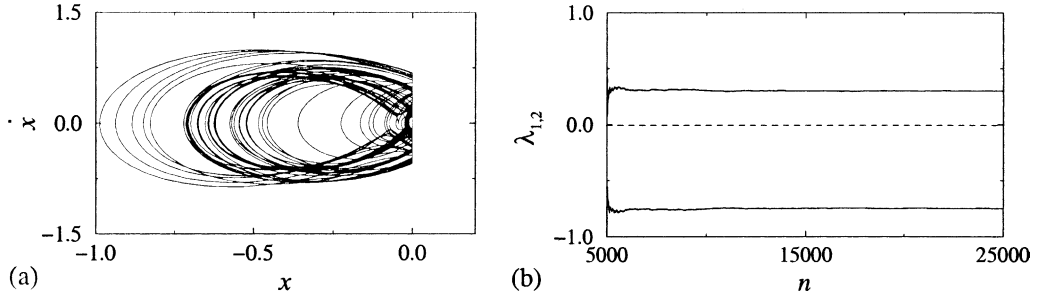

Fig. 8. (a) The phase plane of the chaotic behavior shown in Fig. 2b. (b) The convergent series of the Lyapunov exponents, $\lambda_{1,2}$.

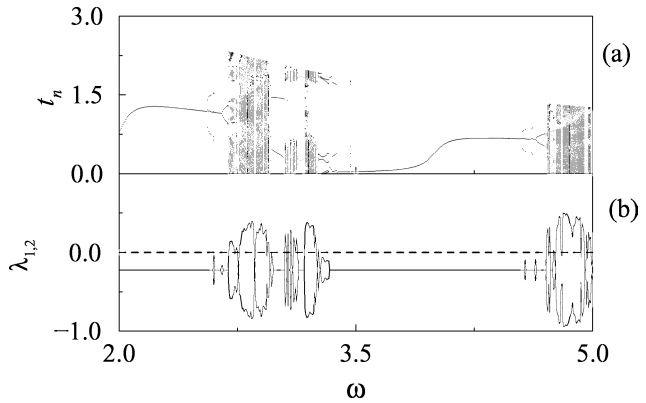

Fig. 9. For the control parameters $\alpha = 1.0$, $r = 0.8$, and $x_c = 0$ of the impact oscillator. (a) Bifurcation diagram of the time t_n (mod $2\pi/\omega$) just before the impact as a function of the excitation frequency ω. (b) The Lyapunov exponents $\lambda_{1,2}$ as a function of ω.

quency ω. For each point the largest Lyapunov exponent is calculated and marked with respect to a linear grade gray scale indicated in the figure. We consider a transient with 1000 iterations and use 5000 iterations for the calculation of the exponents. This diagram is useful tool in studying the dynamical behavior of non-linear systems and, in this case, can be constructed easily because our algorithm is obtained from a map. Thus, using Lyapunov exponents we can discriminate regions characterized by periodic or chaotic motion. Consequently, we can identify bifurcation transitions on the border of these regions.

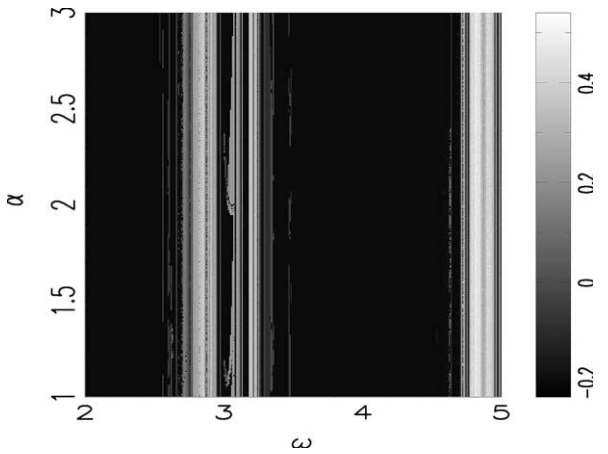

Fig. 10. The largest Lyapunov exponents of the impact oscillator for the amplitude α versus frequency ω with $r = 0.8$ and $x_c = 0$.

3.2. Impact-pair system

In this section we present the numerical results of the Lyapunov exponents for the impact-pair system. The pictures here are constructed in the same way of the pictures shown in previous section.

In this case, the components of the Jacobian matrix derived from transcendental maps are

$$\frac{\partial t_{n+1}}{\partial t_n} = -\frac{1}{\dot{y}_{n+1}}[r\dot{y}_n + \ddot{e}(t_n)(t_{n+1} - t_n)]$$
$$\frac{\partial t_{n+1}}{\partial \dot{y}_n} = \frac{r}{\dot{y}_{n+1}}(t_{n+1} - t_n)$$
$$\frac{\partial \dot{y}_{n+1}}{\partial t_n} = -\frac{\partial t_{n+1}}{\partial t_n}\ddot{e}(t_{n+1}) + \ddot{e}(t_n)$$
$$\frac{\partial \dot{y}_{n+1}}{\partial \dot{y}_n} = -\frac{\partial t_{n+1}}{\partial \dot{y}_n}\ddot{e}(t_{n+1}) - r$$

As mentioned earlier, the source of excitation can be given by a periodic function or a chaotic displacement. First of all, we consider the periodic case, in such situation, $e(t) = \alpha \sin(\omega t)$.

In Figs. 11 and 12, we present the phase planes and their respectives Lyapunov exponents for the periodic attractor (shown in Fig. 4) and the chaotic attractor (Fig. 5). We note once more the convergences of the series occur with good precision.

Fig. 13 shows a bifurcation diagram (Fig. 13a) and Lyapunov exponents (Fig. 13b). In this figure, we can see there is again an excellent agreement between the attractors shown in bifurcation diagram and their corresponding largest Lyapunov exponents values.

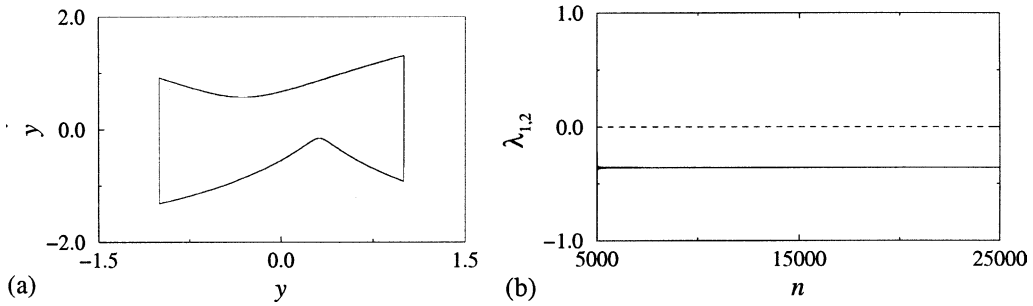

Fig. 11. (a) The phase plane of the periodic behavior shown in Fig. 4. (b) The convergent series of the Lyapunov exponents, $\lambda_{1,2}$.

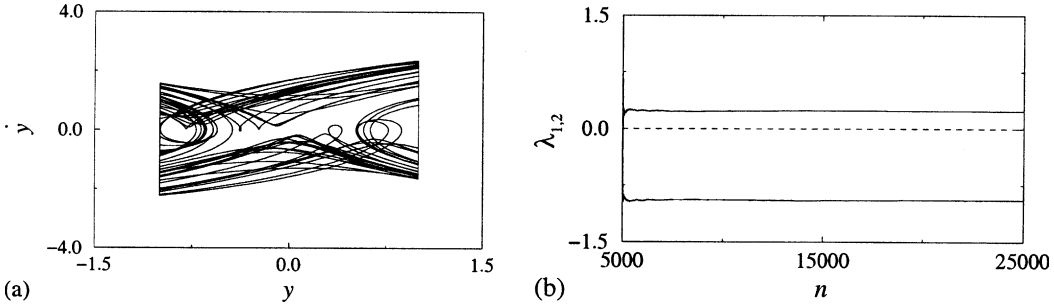

Fig. 12. (a) The phase plane of the chaotic behavior shown in Fig. 5. (b) The convergent series of the Lyapunov exponents, $\lambda_{1,2}$.

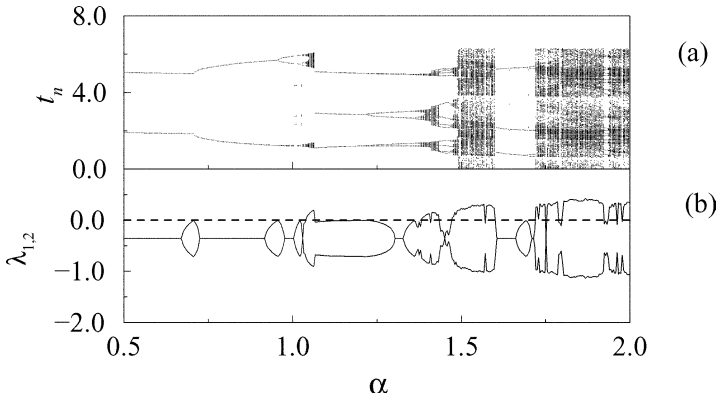

Fig. 13. The impact pair with $e(t) = \alpha \sin(\omega t)$ ($\omega = 1.0$, $v = 2.0$, and $r = 0.7$). (a) Bifurcation diagram of the time t_n (mod 2π) just before the impact as a function of the excitation amplitude α. (b) The Lyapunov exponents $\lambda_{1,2}$ as a function of α.

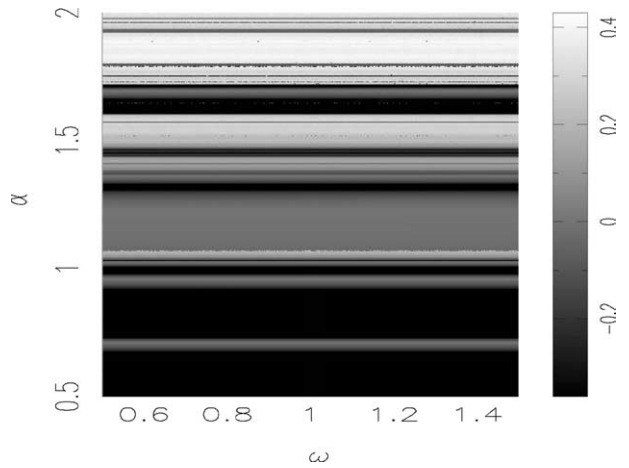

Fig. 14. The largest Lyapunov exponents of the impact pair ($e(t) = \alpha \sin(\omega t)$) for the amplitude α versus frequency ω with $r = 0.7$ and $v = 2.0$.

Figs. 14 and 15 show the diagrams of the largest Lyapunov exponents in the control parameter space. We construct these figures using amplitude α versus frequency ω (Fig. 14) and amplitude α versus coefficient of restitution r (Fig. 15)

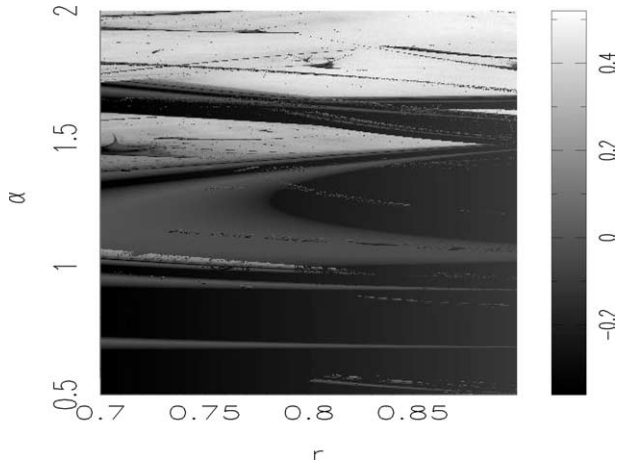

Fig. 15. The largest Lyapunov exponents of the impact-pair ($e(t) = \alpha \sin(\omega t)$) for the amplitude α versus coefficient of restitution r with $\omega = 1.0$ and $\nu = 2.0$.

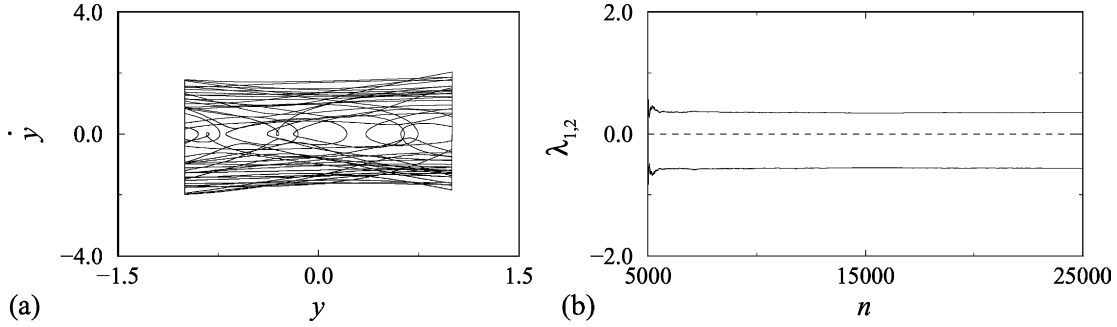

Fig. 16. (a) The phase plane of the chaotic behavior shown in Fig. 6. (b) The convergent series of the Lyapunov exponents, $\lambda_{1,2}$.

as control parameters. In these figures we can descriminate regions of periodic and chaotic attractors, as well as the transition attractors in the parameter space.

Finally, we present an interesting result to show the versatility of the algorithm proposed. Now we consider the impact-pair system with a chaotic excitation. In this case, as we have seen in Fig. 6 the displacement of point mass m is limited by chaotic movable boundaries. Therefore, the only possible solution is a chaotic attractor. In Fig. 16a we show the phase plane for this behavior. In Fig. 16b we plot the test of the convergent series of Lyapunov exponent values, where we can see the convergence occurs with a good precision and there is one positive Lyapunov exponent as expected.

4. Conclusion

In this work we consider a model based algorithm for the calculation of the spectrum of the Lyapunov exponents of attractors of mechanical systems with impacts. To implement this algorithm we need a transcendental map that takes into account the solutions of the integrable differential equations, between impacts, supplemented by transition conditions at the instants of impacts.

We apply this procedure to calculate the spectrum of the Lyapunov exponents of an impact oscillator and an impact-pair system. To show the method precision, for large parameters range, we use the calculated Lyapunov exponents to classify attractors observed in bifurcation diagrams. In addition, we characterize the system dynamics by the largest Lyapunov exponent diagram in the parameter space. Thus, we identify regions of attractors and bifurcation transitions on the border of these regions. Finally, we show that the proposed algorithm can be used for systems with impacts driven by periodic or chaotic excitations.

Acknowledgement

This work is partially supported by the Brazilian Government Agencies FAPESP and CNPq.

References

[1] Oseledec VI. A multiplicative ergotic theorem: Lyapunov characteristic numbers for dynamical systems. Trans Moscow Math Soc 1968;19:197–231.
[2] Blazejczyk-Okolewska B, Kapitaniak T. Co-existing attractors of impact oscillator. Chaos, Solitons & Fractals 1998;9(8):1439–43.
[3] Blazejczyk-Okolewska B, Brindley J, Kapitaniak T. Practical riddling in mechanical systems. Chaos, Solitons & Fractals 2000;11:2511–4.
[4] Blazejczyk-Okolewska B. Analysis of an impact damper of vibrations. Chaos, Solitons & Fractals 2001;12:1983–8.
[5] Guckenheimer J, Holmes P. Nonlinear oscillations, dynamical systems, and bifurcations of vector fields. New York: Springer-Verlag; 1983.
[6] Lichtenberg AL, Lieberman MA. Regular and chaotic dynamics. New York: Springer-Verlag; 1992.
[7] Eckmann JP, Ruelle D. Ergotic theory of chaos. Rev Mod Phys 1985;57:617–56.
[8] Müller P. Calculation of Lyapunov exponents for dynamics systems with discontinuities. Chaos, Solitons & Fractals 1995;5(9):1671–81.
[9] Stefanski A. Estimation of the largest Lyapunov exponent in systems with impacts. Chaos, Solitons & Fractals 2000;11:2443–51.
[10] Stefanski A, Kapitaniak T. Estimation of the dominant Lyapunov exponent of non-smooth systems on the basis of maps synchronization. Chaos, Solitons & Fractals 2003;15:233–44.
[11] Galvanetto U. Numerical computation of Lyapunov exponents in discontinuous maps implicity defined. Comput Phys Commun 2000;131:1–9.
[12] Nordmark AB. Non-periodic motion caused by grazing incidence in an impact oscillator. J Sound Vib 1991;145(2):279–97.
[13] Hinrichs N, Oestreich M, Popp K. Dynamics of oscillators with impact and friction. Chaos, Solitons & Fractals 1997;8(4):535–58.
[14] Han RPS, Luo ACJ, Deng W. Chaotic motion of a horizontal impact pair. J Sound Vib 1995;181(2):231–50.
[15] de Souza SLT, Caldas IL. Basins of attraction and transient chaos in a gear-rattling model. J Vib Control 2001;7(6):849–62.
[16] Hénon M. A two-dimensional mapping with a strange attractor. Commun Math Phys 1976;50:69–77.
[17] Schuster HG. Deterministic chaos: an introduction. New York: VCH; 1988.
[18] Alligood KT, Sauer TD, Yorke JA. Chaos an introduction to dynamical systems. New York: Springer-Verlag; 1997.
[19] Ott E. Chaos in dynamical systems. New York: Cambridge University Press; 1993.